Available online at www.sciencedirect.com

ScienceDirect

IFAC PapersOnline CONFERENCE PAPER ARCHIVE

IFAC PapersOnLine 53-2 (2020) 12708–12713

Active Power Control based on Hydrogen Availability in a Storage Power Plant

Nayeemuddin Ahmed, Paul Gerdun, Harald Weber

Electrical Energy Supply (EEV), University of Rostock, Rostock 18059, Germany

E-mail: (nayeemuddin.ahmed, paul.gerdun, harald.weber)@uni-rostock.de

Abstract: The concept of Electrical Energy Storage (EES) has progressively gained prominence as a means to large-scale integration of intermittent Renewable Energy Sources (RES). The Storage Power Plant (SPP), which uses hydrogen as its primary fuel, is one such solution that can autonomously supply or store electrical energy in bulk according to the requirements of the network. Previous investigations have verified the ability of such a power plant to provide the required ancillary services in order to ensure a secure electrical power supply system. However, one aspect that has remained untested is the effect of diminishing or excess stored hydrogen on the operation of this power plant. In practice, the SPP can be exposed to such extreme situations when it is required to generate or store energy for long periods. Thus, in this paper, a controller model has been recommended which can protect the SPP system when the hydrogen mass in its storage reaches alarming levels. Based on the control mechanism, whenever the hydrogen mass in its storage is about to surpass the upper or lower permissible limits, the SPP can seamlessly transition from one mode to another and adjust its power output. This enables the SPP to regulate the level of its stored hydrogen mass.

Keywords: Ancillary service, energy storage, hydrogen storage, renewable integration, security.

1. INTRODUCTION

To meet the EU 2020 climate and energy targets, 18% of Germany's gross final energy consumption (approximately 2500 TWh) needs to originate from renewable energy sources (RES) (European Commission (2020); German Environment Agency (2020)). The country is well on course, generating 17.1% of this energy from renewables in 2019 (BMWi (2020)). However, by 2050, this figure is expected to be around 60% (IEA (2020)). Such high penetration of renewable energy (primarily wind and solar for Germany), though deemed necessary for climate protection, is introducing additional challenges in regulating the electrical energy supply system. This includes higher frequency fluctuations, presence of harmonics, as well as increased forecast errors (Liang (2016)).

One of the main problems with RES is that their ability to generate electrical power is dependent on the fluctuating primary resource, i.e. sun and wind. As a result, such resources cannot be used to meet the power requirements in the grid at all times or provide the required balancing energy with 100% reliability (Chuang and Schwaegerl (2009)). Currently, the difference between varying electrical power generation by RES and consumption by loads is bridged by conventional power plants (CPP). In the future though, most of these CPPs are planned to be shut down and replaced by renewables both due to lack of fossil fuels and to meet climate action targets (German Institute for Economic Research (2019)). Hence, the potential for alternative solutions which can provide the same ancillary services as CPPs is becoming increasingly important.

One such solution is the Storage Power Plant (SPP), which consists of an interconnected system of converters and storages. The arrangement of the components inside this power plant ensures that it can supply electrical energy as per the grid requirement as well as store it during excess infeed from RES. The SPP can perform this function over long periods depending on the size of its storages. There are three such primary storages inside the SPP, i.e. supercapacitor, battery and hydrogen storage. Each of these is ideally suited for its respective purpose of providing instantaneous reserve, primary and secondary control, thus enabling the SPP to meet the necessary ancillary service requirements (Gerdun et al. (2019)).

An increasing share of RES substituting CPPs leads to reduced grid inertia. To overcome this problem, an inertia independent governing principle can be used in electrical grids of the future. Such a form of ancillary service is called Nodal Voltage Angle Control. The coherent operation of SPPs with CPPs under this principle has already been exhibited (Weber et al. (2018); Weber et al. (2019)). However, the behavior of a SPP once its stored hydrogen level reaches the upper or lower threshold has remained unexplored. Thus, in this paper a control mechanism has been proposed which always regulates the stored hydrogen

⋆ Research project - "Netz-Stabil", financed by the European Social Fund (**ESF/14-BM-A55-0025/16**)

10.1016/j.ifacol.2020.12.1865

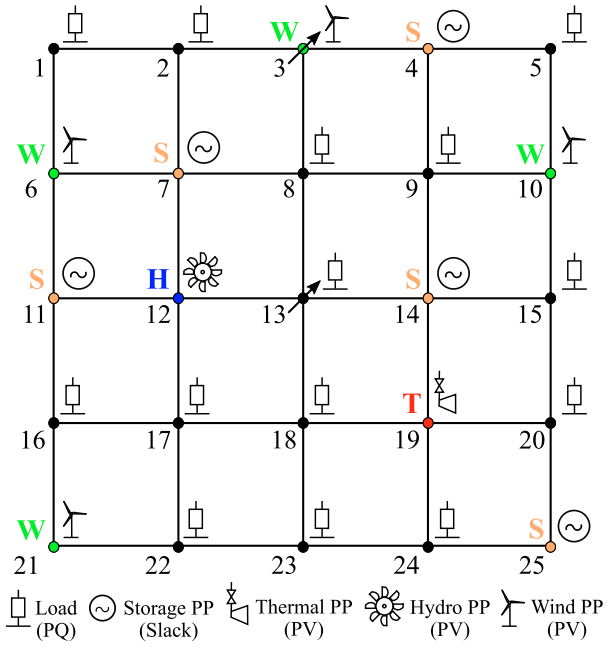

Fig. 1. 25 node electrical network

inside the SPP between permissible levels. The operation and associated results of this method are discussed in the following sections of the paper.

2. TEST ELECTRICAL NETWORK

The test bench for the investigations is shown in Fig. 1. The network consists of 25 equidistant nodes, each connected to either a power plant or a load. The nodes are interconnected via transmission lines, each 250 km long and at a voltage level of 110 kV. The line impedances are equal in magnitude with a resistance to reactance ratio of 0.1. Such a squared grid is used to easily highlight the principles of power production of the four different kinds of power plants present in the test bench. This will become more apparent once Fig. 5 is analyzed.

There are eleven power plants, of which five are slack SPPs (S), i.e. converters at terminals where the voltage magnitude ($|V|$) and angle (ϕ_u) are kept constant. Out of the other six, four represent wind power plants (W), while the other two each denote a conventional hydroelectric (H) and a coal fired thermal (T) power plant. The CPPs are represented by PV terminals, where the active power (P) and voltage magnitude ($|V|$) are controlled. The four wind power plants (WPPs) and remaining 14 nodes, each housing a load, are represented by PQ terminals where the active (P) and reactive power (Q) consumed are known.

The network modeling and RMS simulations are performed in the software DIgSILENT PowerFactory. The base power value of the per-unit-system is selected as 10 MVA. The initial load flow setpoints for the different power plants are summarized in Table 1. Each load also consumes 3.3 MVAR of reactive power which is supplied by the power plants. Unfortunately, the reactive power results and control methods are not included in this paper due to space constraints.

Table 1. Initial working points of the different power plants and loads

Type	No.	Power per PP (MW)	Total power (MW)
Thermal power plant	1	23.51	23.51
Hydro power plant	1	23.51	23.51
Wind power plant	4	23.52	94.08
Storage power plant	5	0	0
Total generation	-	-	**141.1**
Load	14	10	140
Losses	-	-	1.10
Total consumption	-	-	**141.1**

3. INTERNAL SPP STRUCTURE

As seen in Fig. 2, the SPP consists of three main storages; the supercapacitor, battery and hydrogen storage. These storages have different energy capacities and are responsible for providing instantaneous reserve, primary and secondary control response respectively. There are DC-DC converters which control the power flow between the storages. All components operate in DC mode. Hence, the power plant uses a DC-AC converter for grid connection. The SPP structure used in the simulation software, models the control scheme of the DC-DC converters which govern the power flow between the SPP storage components.

The first storage, i.e. the supercapacitor, is directly connected to the DC-AC converter. Depending on the type of disturbance in the network, the supercapacitor immediately supplies instantaneous reserve to the grid or stores it from the grid. It can immediately charge and discharge with a high power gradient and additionally has an almost infinite lifetime because of its electrostatic energy storage principal. These properties make it ideal for its task of providing instantaneous response. Hence, its behavior is analogous to the rotating mass in a turbine shaft of a conventional thermal power plant (TPP).

The second storage, i.e. the battery, connected in parallel to the supercapacitor, supplies or stores primary control power, in order to compensate for the low energy density of the supercapacitor. This process is controlled by the DC-DC converter between these two components. In contrast to a supercapacitor, the battery is optimally suited for the purpose of providing primary control power. This is due to its electrochemical energy storage principle which allows it to possess a higher energy storage density compared to a supercapacitor and a preferably lower charging and discharging gradient, to improve its lifetime. Thereby, it represents the equivalent of the steam boiler in a conventional TPP.

As the third main storage, the hydrogen storage is responsible for supplying secondary control power, similar to the coal storage in a coal fired TPP. Additionally, it can store secondary control power. Depending on the power flow direction, either a fuel cell or an electrolyser is used to empty or refill the hydrogen storage. The power flow for

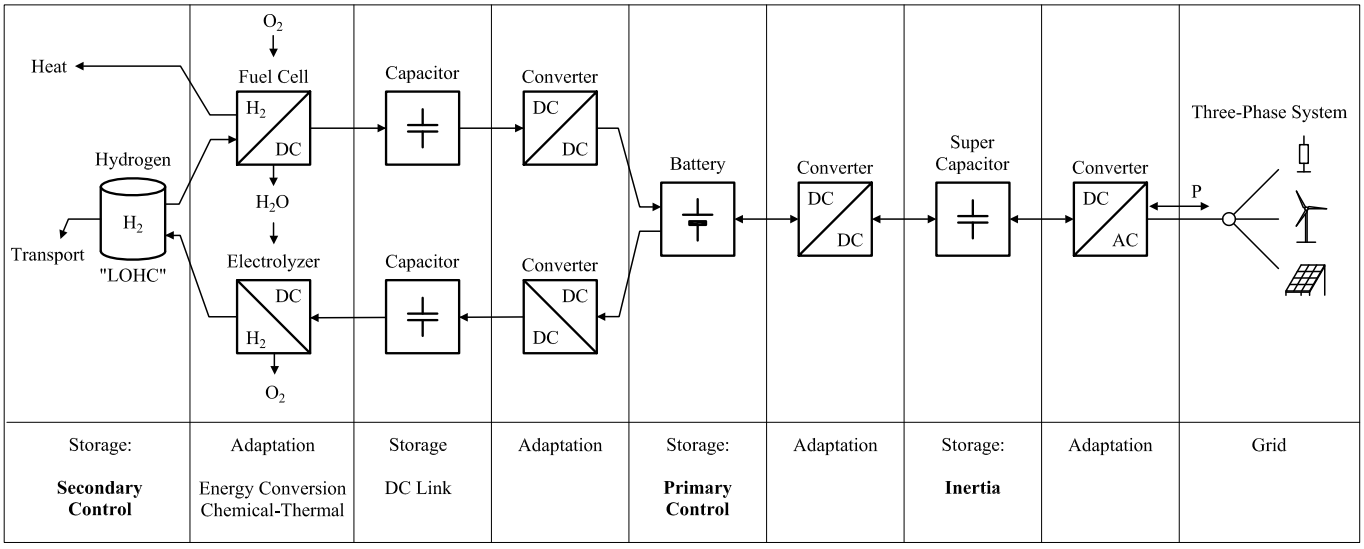

Fig. 2. Working principle of the internal components of a storage power plant (SPP)

each of these cases is controlled by the DC-DC converter in the respective paths between the hydrogen storage and the battery. Each of these two DC-DC converters possesses a DC link buffer storage. The behavior of these capacitors is analogous to the steam boiler pipe wall in a TPP.

While utilizing the hydrogen storage, the fuel cell generates electrical energy from the chemical reaction between stored hydrogen (H_2) and external oxygen (O_2). One by-product of this reaction is thermal energy which can be used for district heating. Another product is dihydrogen monoxide (H_2O). In case of a reversed power flow, the H_2O can in turn be used as the electrolyte to generate hydrogen as well as oxygen as a by-product. The hydrogen can then be stored in a Liquid Organic Hydrogen Carrier (LOHC) system. Such a system enables safe, easy storage and transportation of hydrogen at a high energy density under ambient conditions, using the currently available infrastructure (Teichmann et al. (2011)). In addition to being used for electrical power generation in the SPP, the stored hydrogen can also be utilized in other applications, for example in automobiles.

4. ANGLE CONTROLLER MODEL

The active power of the SPP needs to be controlled for two reasons:

(1) Delivering controlled power to the grid
(2) Protecting the power plant from overcurrent and voltage fluctuations beyond permissible limits

These criteria are satisfied by the angle controller of the SPP, which is able to control the active power generation of the power plant via the voltage angle (ϕ_U) at its connection terminals. As described in the process flow diagram in Fig. 3, once the active power and stored hydrogen mass are within permissible limits, the SPP can be run by the operator in either Slack or PQ mode. This choice is also influenced by the power demand on the electrical network.

In slack mode, the SPP keeps its voltage angle constant (grid former) and uses the difference to the voltage angles of the surrounding load nodes to produce more power. This is more evident in the analysis of Fig. 5 and 6. If the plant operator decides to run the SPP at constant active power, it's switched to PQ mode to allow the converter system function as a grid follower instead. If either the power output or the stored hydrogen mass surpasses the implemented thresholds, the SPP automatically switches to Emergency PQ mode as a protective measure to lower its power output. Under such circumstances, the operator can also shut the power plant down, if necessary. The SPP will continue to remain in this Emergency PQ mode, until its stored hydrogen mass returns to acceptable levels and its power output is within corresponding bounds which includes the hysteresis band (Δ). Then, the SPP can function in either mode again.

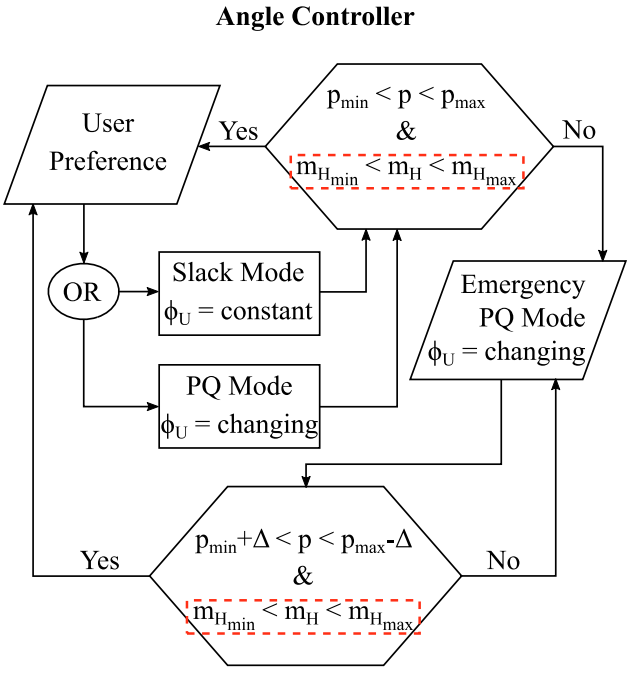

Fig. 3. Process flow of the angle controller

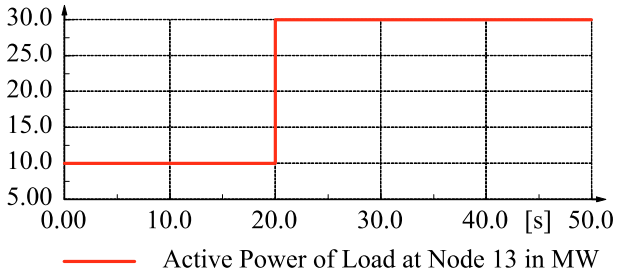

Fig. 4. Step increase in the active power consumption by the load at node 13

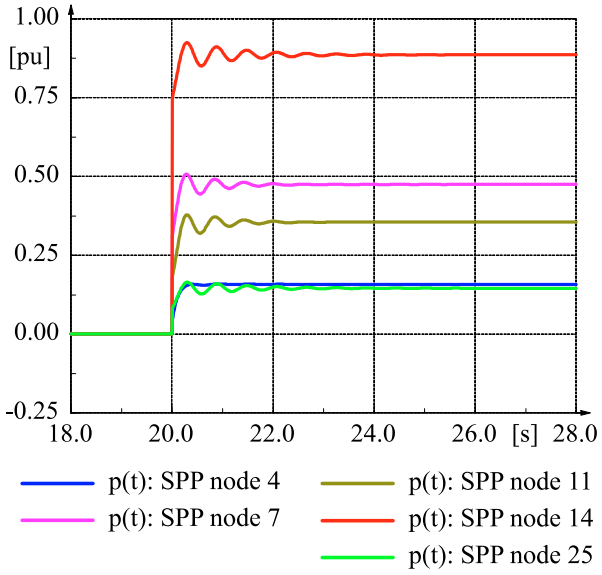

Fig. 5. Response of the SPPs to increased power demand

5. RESULTS AND OBSERVATION

The first case of investigation involves applying a step increase in the power demand of the load at node 13. As a result, the power consumption at the central node increases from 10 MW to 30 MW at 20 s, shown in Fig. 4. To meet the increased power demand in the network, the five SPPs respond immediately and start generating more active power. The magnitude of this power increase depends on the electrical proximity of a particular SPP to the origin of the disturbance, i.e load at node 13. The closer the SPP to the central node, the greater is the increase in its power output, as shown in Fig. 5. Due to the resistance in the transmission lines, there will be some losses during the power flow and the total additional power supplied by the SPPs will be greater than the power demand increase of the load at node 13. The CPPs at nodes 12 and 19 as well as the wind turbines at nodes 3, 6, 10 and 21, act as PV nodes in this case and keep their power output constant.

Taking the positions of slacks in the network into account, generally the voltage angles change more for the loads closer to the source of the disturbance. Hence, as exhibited in Fig. 6 the voltage angle values are higher near to node 13 and progressively decrease towards the periphery of the grid. On the other hand, the voltage angles of the slacks are constant. This increased difference between the voltage angles enables the slacks to produce more power closer to

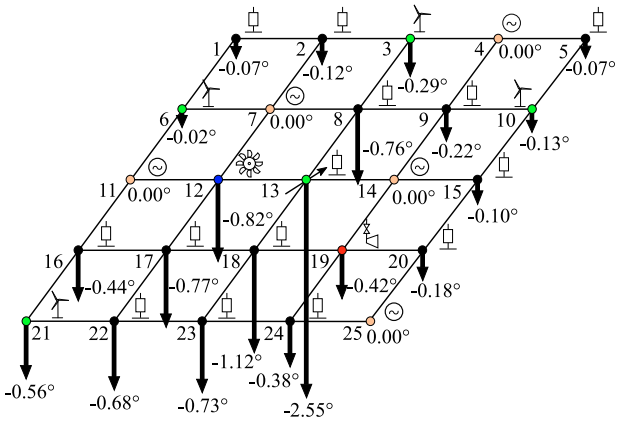

Fig. 6. Changes in nodal voltage angles due to the step increase in power demand at node 13

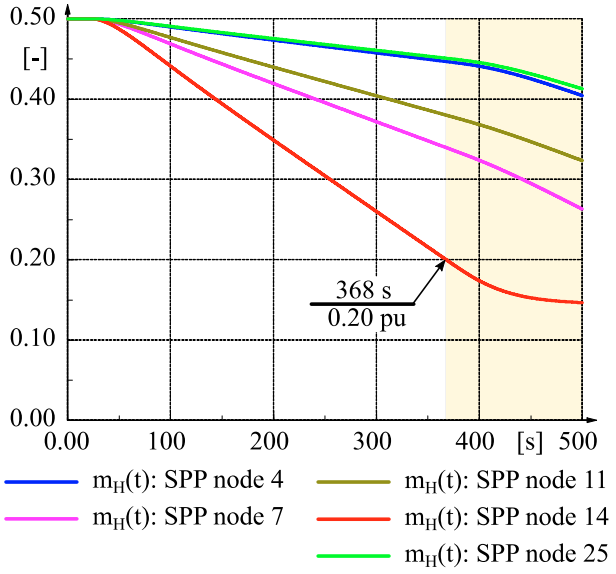

Fig. 7. Decrease in the stored hydrogen mass of all the SPPs due to continuous generation of active power

the point of demand. These trends in active power output and voltage angle changes are pronounced due to the use of a squared grid, as shown in Fig. 1. In a grid with a non-uniform distribution of the line impedances, it would not be as easy to highlight the principles of power production with such clarity when the SPPs are being governed by voltage angle control.

As the SPPs continue to provide active power, the mass of hydrogen in their respective storages reduce, as shown in Fig. 7. Since the SPP at node 14 is producing more active power than the others, the rate of hydrogen mass flow from its storage is also the highest. To prevent the hydrogen store from being completely exhausted within a short time, a droop control mechanism is installed, which lowers the power output of the SPP once its hydrogen mass falls below a given lower limit. For our investigations, this limit has been set to 20%. Thus, when the hydrogen mass of the SPP at node 14 surpasses this limit at 368 s, the SPP switches from slack to the Emergency PQ mode and the droop controller output, (p_{H_2}), starts transmitting a negative value and lowers the scheduled power flow of the power plant, as displayed in Fig. 8.

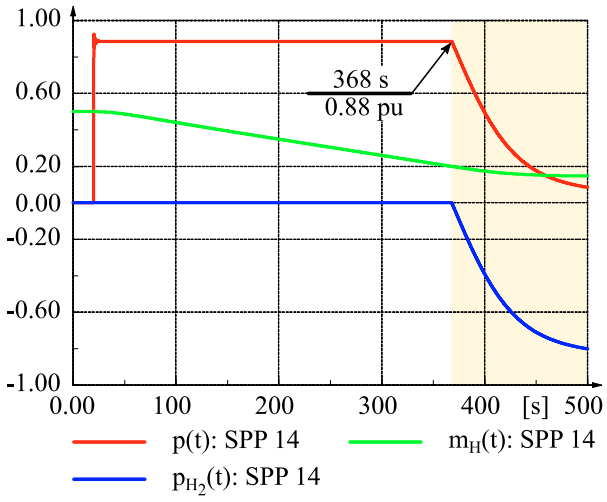

Fig. 8. Relation between the hydrogen mass and active power output of the SPP at node 14

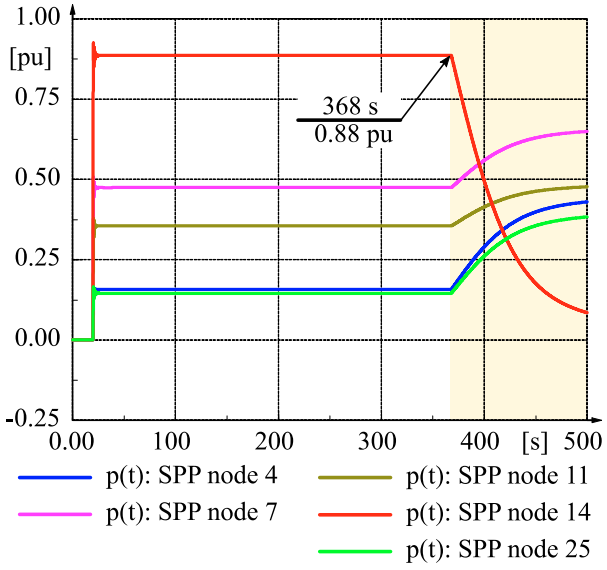

Fig. 9. Change in output power when the hydrogen mass in the SPP at node 14 crosses its lower limit

To compensate for this decrease in the output power of the SPP at node 14, the four other SPPs in the grid increase their power generation. The next nearest slack to node 13, SPP at node 7, now generates the highest power. However, the magnitude of the power increase does not only depend on the electrical proximity of a SPP to node 13, but also on the mass of hydrogen remaining in its storage. Hence, as shown in Fig. 9, the SPPs at nodes 4 and 25 despite being the two farthest SPPs from node 13, exhibit a greater increase in power output since they have more hydrogen remaining in their storage. Furthermore, the voltage angle of the SPP at node 14 starts to decrease once it switches to Emergency PQ mode. This allows it to lower its power output setpoint, as illustrated in Fig. 10. The four other SPPs continue to function as slacks and thus keep their voltage angles constant.

For the second investigation, a ramp is applied to increase the active power generation of the WPP at node 3 by 15 MW between 100 s and 200 s. This is done to test

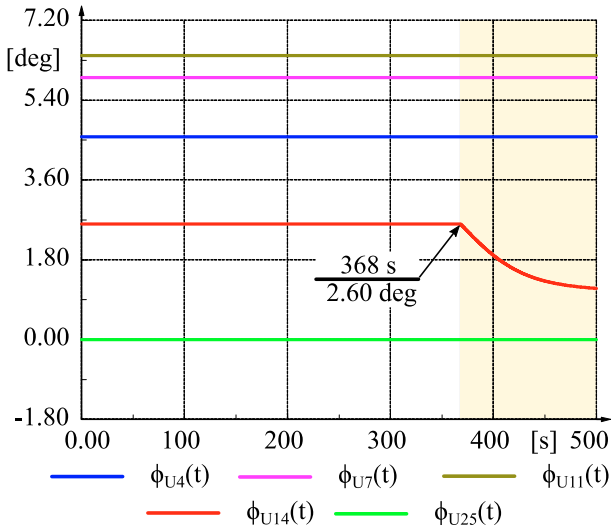

Fig. 10. Change in voltage angle when the hydrogen mass in the SPP at node 14 crosses its lower limit

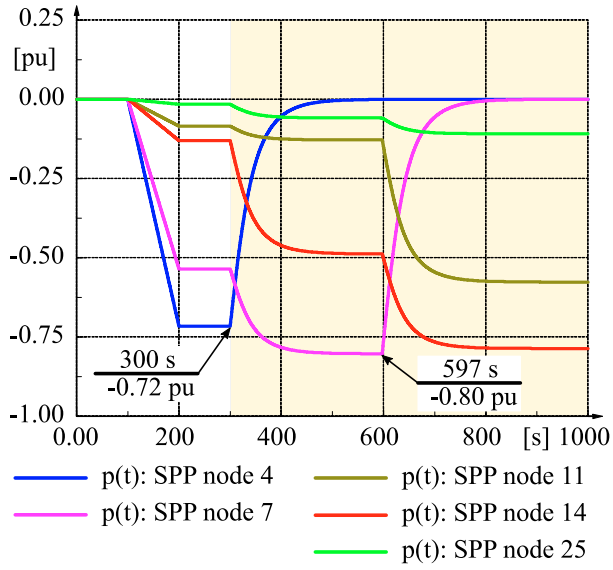

Fig. 11. Change in output power when the hydrogen mass in the SPPs at node 4 and 7 crosses its upper limit

the energy storing capability of the SPPs and study their behavior once their secondary storage contains excess hydrogen. For this investigation, the initial power plant setpoints as denoted in Table 1, are retained. As shown in Fig. 11, all the SPPs start in slack mode and are storing energy with the onset of the wind ramp, thus exhibiting a negative active power output. Since the SPP at node 4 is closest among the SPPs to the WPP at node 3, it stores energy at the fastest rate.

As opposed to the previous case, the initial levels of stored hydrogen mass in the respective SPPs are assigned different values to observe its effect on the energy storing capability of a SPP. Since all the SPPs are storing energy in slack mode, the mass of hydrogen in their respective storages increase, as shown in Fig. 12. To prevent the mass of hydrogen in the storage from exceeding the upper permissible limit of 80%, the SPP at node 4 transitions from slack to Emergency PQ mode at 300 s. Once again,

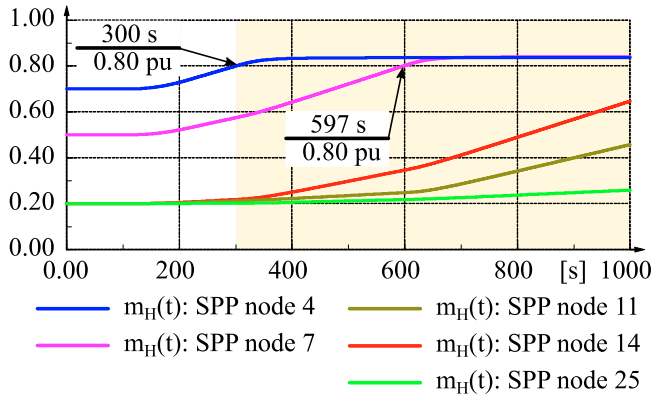

Fig. 12. Increase in the hydrogen mass of all the SPPs

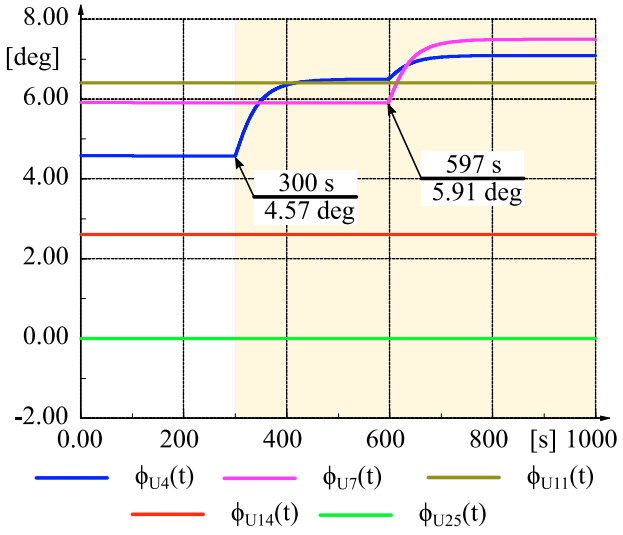

Fig. 13. Change in voltage angle when the hydrogen mass in the SPPs at node 4 and 7 crosses its upper limit

a droop control mechanism is used with the controller output, (p_{H_2}), this time generating a positive value. This returns the scheduled power flow of the power plant to 0 MW. Consequently, the four other SPPs start to store energy at a faster rate, which also increases the rate of hydrogen mass flow into their individual storages. At 597 s, this leads to the SPP at node 7 exceeding the upper threshold of hydrogen mass storage as well and switching from slack to Emergency PQ mode. This causes its power output to gradually return to 0 MW as well, leaving the three other SPPs to fulfill the network storage demand.

When the SPP at node 4 switches from slack to Emergency PQ mode at 300 s, its voltage angle increases to allow its power output to change, as exhibited in Fig. 13. The same phenomenon is observed when the SPP at node 7 reaches its storage limit at 597 s. During this time, as storage support from the SPP at node 7 ceases, the voltage angle of the SPP at node 4 increases further to maintain its power output at 0 MW. The SPPs at nodes 11, 14 and 25 continue to keep their voltage angle constant since they remain in slack mode.

6. CONCLUSION

This paper presented the control mechanism by which the mass of hydrogen present in the storage of the SPP can always be maintained within permissible levels. This was achieved by the SPP switching autonomously from slack to Emergency PQ mode at the threshold values and using the proposed droop control mechanism to regulate its active power output. Additional simulations need to be carried out to test the functionality of this control mechanism in alternate grid configurations. Currently, research is also being dedicated to developing improved reactive power control schemes for the SPP. In addition, more investigations will be required to estimate the total losses as well as the market compatibility of this novel system and hence prepare a quantitative comparative study in relation to the current power system.

ACKNOWLEDGEMENTS

This paper was created within the framework of the research project “Netz-Stabil” and financed by the European Social Fund (**ESF/14-BM-A55-0025/16**). It is part of the qualification program “Promotion of Young Scientists in Excellent Research Associations - Programme for Excellence in Research in Mecklenburg-Western Pomerania”.

REFERENCES

BMWi (2020). Germany on track for meeting eu renewables target.

Chuang, A.S. and Schwaegerl, C. (2009). Ancillary services for renewable integration. In *2009 CIGRE/IEEE PES Joint Symposium Integration of Wide-Scale Renewable Resources Into the Power Delivery System*, 1–1.

European Commission (2020). 2020 climate & energy package.

Gerdun, P., Ahmed, N., Vernekar, V., Töpfer, M., and Weber, H. (2019). Dynamic operation of a storage power plant (spp) with voltage angle control as ancillary service. In *2019 International Conference on Smart Energy Systems and Technologies (SEST)*, 1–6.

German Environment Agency (2020). Renewable energy share in gross final energy consumption and gross electricity consumption.

German Institute for Economic Research (2019). Phasing out Coal in the German Energy Sector. 45.

IEA (2020). International Energy Agency- Germany 2020, energy policy review.

Liang, X. (2016). Emerging power quality challenges due to integration of renewable energy sources. *IEEE Transactions on Industry Applications*, 53(2), 855–866.

Teichmann, D., Arlt, W., Wasserscheid, P., and Freymann, R. (2011). A future energy supply based on liquid organic hydrogen carriers (LOHC). *Energy & Environmental Science*, 4(8), 2767–2773.

Weber, H., Ahmed, N., Töpfer, M., Gerdun, P., and Vernekar, V. (2019). Dynamic behavior of conventional and storage power plants in a single power system. In *2019 IEEE Milan PowerTech*, 1–6.

Weber, H., Baskar, P., and Ahmed, N. (2018). Power system control with renewable sources, storages and power electronic converters. In *2018 IEEE International Conference on Industrial Technology (ICIT)*, 1–7. IEEE.